Brief Articles

Spectroscopic Studies of Diketoacids−Metal Interactions. A Probing Tool for the Pharmacophoric Intermetallic Distance in the HIV-1 Integrase Active Site

Cédric Maurin,[†] Fabrice Bailly,[†] Eric Buisine,[†] Hervé Vezin,[†] Gladys Mbemba,[‡] Jean François Mouscadet,[‡] and Philippe Cotelle*,[†]

Laboratoire de Chimie Organique et Macromoléculaire, UMR CNRS 8009, Université des Sciences et Technologies de Lille, 59655 Villeneuve d'Ascq, France, and Laboratoire de Biotechnologies et Pharmacologie Génétique Appliquée, UMR CNRS 8113, ENS Cachan, 61 Avenue du Président Wilson, 94235 Cachan, France

Received May 10, 2004

The interactions with divalent cations of 4-phenyl-4-oxo-2-hydroxybuten-2-oic acid (benzoylpyruvic acid (BPA)), the pharmacophore of HIV-1 integrase inhibitors, were investigated using spectroscopic tools. In the absence of the enzyme, a 2:2 metal−ligand complex was characterized with an intermetallic distance of 4−6 Å. Molecular modeling allowed us to propose a compatible structure for the metal−ligand complex. BPA does not inhibit the reactions catalyzed by HIV-1 IN, emphasizing the importance of the aromatic ring substitution in the antiviral activity.

Introduction

Integrase (IN) is one of the three enzymes encoded in the HIV-1 genome and is responsible for the integration of viral DNA into host DNA. IN has been recently designed as one of the most important targets in AIDS research.[1] Despite the large number of compounds inhibiting HIV-1 integrase in vitro, only diketoacids (DKAs)[2−5] were found to be active in vivo. Their antiviral activity has been correlated to the inhibition of IN.

Because of their structure, DKAs could simultaneously coordinate two divalent metal ions in the HIV integrase active site, which is consistent with previous structural and biochemical studies of HIV integrases and transposases. Whereas Grober et al.[6] proposed that one molecule of DKA bound to two metals on the same side separated by 3.6 Å, Pommier's group[7] suggested that the two metals are coordinated on the opposite sides of DKAs at about 7 Å. Recently a docking study[8] concluded that the magnesium ion coordinated by the aspartic residues D64 and D116 of the enzyme may interact specifically with the diketo moiety of DKA, while the manganese ion may use two anchorage points: the carboxylic function through one of its two oxygen atoms and the oxygen atom linked to the carbon α position in DKA molecule.

Since DKAs were found to interact with numerous viral enzymes, i.e., HIV-1 integrase,[2,4−8] HIV-1 RNase H,[9] influenza endonuclease,[10] and hepatitis C RNA polymerase,[11] it appears to be of major interest prior to any docking investigation to have the best knowledge on the structure of DKAs in solution and also on their putative cationic binding site(s).

* To whom correspondence should be addressed. Phone: +33-320337231. Fax: +33-320336309. E-mail: philippe.cotelle@univ-lille1.fr.
† Université des Sciences et Technologies de Lille.
‡ ENS Cachan.

The first step of our study was to investigate the structure of BPA in solution in the absence and in the presence of Mg^{2+} ions. The second step was to probe the existence of two simultaneous cationic binding sites of BPA by means of ESR spectroscopy using the paramagnetic Mn^{2+} ion instead of Mg^{2+}, which is diamagnetic. The third step was to confirm the 2:2 stoechiometry of the metallic complexes using mass spectrometry. Theoretical calculations were finally undertaken in order to propose a model of complex structure compatible with the observed spectroscopic data.

^{1}H and ^{13}C NMR Spectroscopy. Structure of BPA in Solution

The ^{1}H and ^{13}C NMR spectra of BPA were recorded in aqueous solution, in buffered aqueous solutions (pH 7.5 and 10), and in the presence of excess $MgCl_2$. At physiological pH, BPA is expected to exist as monoanion BPA^-, the acidity constant of the carboxylic moiety being in the pK_a range 3.5−4.0.[12] Under basic conditions, the enol function also becomes deprotonated, giving the enolate BPA^{2-} (pK_a > 7.6).[12] The ^{1}H and ^{13}C NMR chemical shifts of BPA are reported in Table 1. BPA^- presents the strong characteristic upfield shift of H3 and strong downfield shifts of C5 and C2 due to the formation of the *E*,*Z* form.[13] Under more basic conditions, the chemical shifts of C2 and H3 are strongly attenuated because of the electronic effects of the supplementary negative charge in the dianionic form (highfield shift of C5, downfield shifts of aromatic protons). The chemical shifts obtained at pH 10 or with 1 equiv of $MgCl_2$ are clearly similar, suggesting that Mg^{2+} promotes the formation of the dianionic species BPA^{2-}.

ESR Spectroscopy

The ESR study was carried out in a 5 μM solution of BPA in buffered aqueous solution (pH 7.5), methanol,

10.1021/jm0408464 CCC: $27.50 © 2004 American Chemical Society
Published on Web 09/21/2004

Table 1. ^{1}H and ^{13}C Chemical Shifts (δ in ppm) of the BPA Species Present in H_2O, in Buffered Solution (pH 7.5 and 10), and after Addition of $MgCl_2$

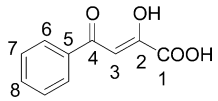

conditions	obsd species	C1	C2	C3	H3	C4	C5	C6	H6	C7	H7	C8	H8
H_2O	BPA	169.9	164.5	99.3	7.10	191.3	135.5	128.8	8.06	130.3	7.59	135.3	7.68
H_2O, pH 7.5	BPA^-	173.0	183.0	94.7	5.60	189.9	141.6	128.6	7.98	134.0	7.52	135.8	7.59
H_2O, pH 10.0	BPA^{2-}	174.5	168.7	97.6	6.75	191.7	137.9	130.4	7.82	130.0	7.39	135.7	7.49
H_2O, Mg^{2+}	BPA^{2-}	174.9	168.8	97.6	6.55	191.9	136.2	130.3	7.84	129.0	7.40	133.9	7.52

or DMSO with variable amounts of Mn^{2+} (the metal−ligand ratio varying between 1/6 and 2). In water, BPA was not able to complex Mn^{2+}. The only observed paramagnetic species was the very stable hexahydrated manganese ion. In organic solvents, two kinds of ESR spectra can be obtained, depending on the metal−ligand ratio. For high metal−ligand ratios (>0.5) six-line spectra were observed with a hyperfine splitting constant A for ^{55}Mn of 91 G (Figure 1, top), characteristic of one Mn^{2+} ion coordinated with BPA (the spectra were different from those of the free Mn^{2+} solution). For low metal−ligand ratios (<0.25) 11-line spectra characteristic of two interacting Mn^{2+} ions were recorded (Figure 1, bottom). This observed spectrum arises from the exchange J constant characteristic of the electronic coupling between the two Mn^{2+} S1 and S2 electronic spins. The 11 lines centered at $g = 2$ indicate a strong exchange with $J \gg A$. The hyperfine splitting constant A for ^{55}Mn of 46 G is at one-half the interval for an isolated previously measured Mn^{2+} ion. From the spectroscopic data, assuming the dipole approximation with the dipolar term equal to $D = -g^2\beta^2/r^3$, the intermetallic distance can be evaluated in the range 4−6 Å.

Mass Spectrometry

For mass spectrometry analysis, a solution of 50 μM BPA and 25 μM magnesium(II) or manganese(II) acetate in methanol was prepared. MALDI (mass-assisted laser desorption ionization) mass spectra were recorded on a Finnigan MAT Vision 2000 (Bremen). Three characteristic peaks at m/z 487 (20%), 488, and 489 with relative ratios of 1/0.3/0.3 were observed in the presence of Mg^{2+}, and a significant one at m/z 549 (10%) was observed in the presence of Mn^{2+} corresponding to the dimeric metal−ligand $[2M^{2+}-2(BPA^{2-})-2H_2O-Na^+]$ ions.

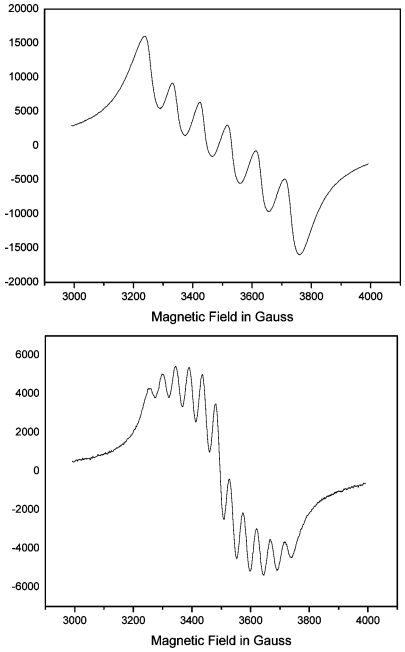

Figure 1. 9 GHz ESR spectra of Mn^{2+} in methanol solution in the presence of **1** with a metal−ligand ratio of 1/2 (top) and 1/6 (bottom). Experimental setting was 5 mW microwave power and 5 G amplitude modulation.

Modeling of Metal−Ligand Complexes

The stability of the two dimeric metal−ligand model structures compatible with the assumptions given below was investigated using quantum chemistry calculations. Only magnesium (closed-shell system) metal was considered. We assumed that (i) each ligand molecule is in its dianionic form, (ii) Mg^{2+}−ligand interactions are not mediated by water molecules, (iii) the BPA^{2-} molecules possess two possible sites of interaction with Mg^{2+}, where the first site involves one of the two oxygen atoms of the carboxylate group and the second site involves the two oxygen atoms of the keto−enolate moiety, (iv) as usually observed, Mg^{2+} ion is considered to be in an octahedral symmetry in its first coordination shell, (v) to form symmetrical dimeric complexes, each magnesium atom can bind to the first site of one BPA^{2-} molecule and the second site of the other BPA^{2-} molecule, (vi) to complete the first octahedral coordination shell of each magnesium atom, three water molecules were added, giving a total of six water molecules in the entire complex structure.

Ab initio calculations were carried out using the Gaussian 98 suite of programs.[14] The geometry of the free BPA^{2-} ligand was first optimized at the Hartree−Fock level of theory using the 6-31G* basis set. Then two putative dimeric Mg^{2+}−ligand structures were built and fully optimized at the same level of theory. A single-point density functional theory (DFT) calculation using the B3LYP functional hybrid method was finally performed.

The two dimeric Mg^{2+}−ligand structures compatible with our assumptions correspond to a folded (Figure 2a) and an unfolded (Figure 2b) geometry. At the HF/6-31G* and B3LYP/6-31G* levels, the folded structure is the most stable, with 6.3 Å separating the centers of the two aromatic rings (11.9 Å in the unfolded geometry). The differences in energies are 4.1 and 9.7 kcal/mol at the HF and B3LYP levels, respectively. The intermetallic distance calculated in the optimized geometries is in accordance with the 4−6 Å range deduced from the ESR spectroscopy study of related Mn^{2+}−ligand complexes. The distance between the two mag-

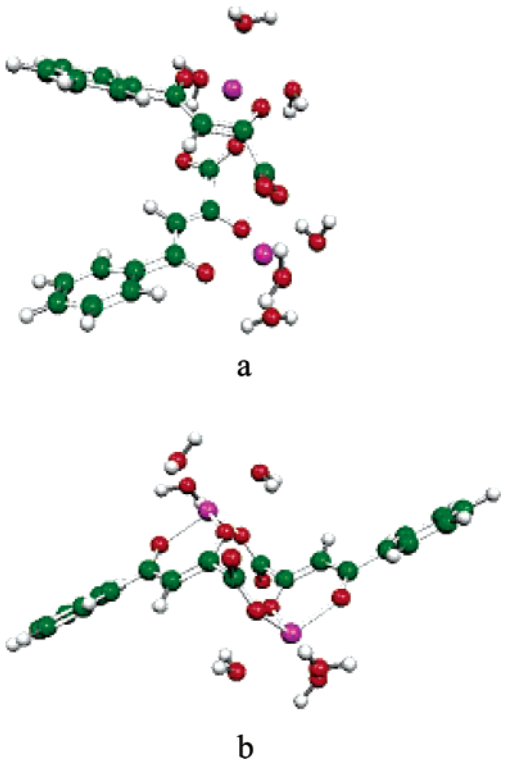

Figure 2. Structure of stacked (a) and unstacked (b) 2:2 Mg^{2+}−BPA^{2-} dimers optimized with the DFT B3LYP/6-31G* formalism.

nesium atoms is 5.3 Å in the folded structure of Figure 2a and 5.5 Å in the unfolded structure of Figure 2b.

HIV-1 Integrase Inhibition

BPA was screened for inhibitory activity against HIV-1 IN in both Mg^{2+}-dependent 3′-end-processing and strand transfer reactions as described earlier.[15] BPA does not inhibit HIV-1 IN at concentrations up to 100 μM, whereas it was found to inhibit strand transfer with an IC_{50} of 25 μM using Mn^{2+} as a divalent cation source.[7] These results are consistent with the previously observed metal-dependent IN inhibition of DKAs.

Discussion

Crystallographic data of the catalytic domain of IN reveal a single binding site for Mg^{2+}, whereas in avian sarcoma virus (ASV) IN, an additional metal coordinated by aspartic D64 and glutamic E157 was observed with Zn^{2+} or Cd^{2+} ions.[16] The intermetallic distances are 3.62 and 4.06 Å, respectively. Similarly, the crystal structure of the HIV-1 RNase H domain of the HIV-1 reverse transcriptase also shows the existence of two Mn^{2+} ions coordinated concurrently by the DDE motif[17] in the active site, with a Mn−Mn distance of about 4 Å. NMR experiments on the same enzyme in the presence of increasing amounts of Mg^{2+} revealed two discrete binding sites largely unoccupied under physiological conditions in the absence of DNA substrate.[18] In the absence of definitive proof of the exact nature, number, and function of the divalent cations in the active site, the catalytic domain of HIV-1 IN is considered to bind two Mg^{2+} ions.[19]

A direct interaction of DKA with divalent metal in the IN active site has been proposed using functional and binding assays,[8] and hence, the sequestration of the divalent cation by DKA could be responsible for IN inhibition. Pharmacophoric modifications have also shown that the free acidic function is essential for the activity. It was therefore of prime interest to know the ionic state of BPA under physiological conditions and to characterize its interactions with divalent cations.

In this paper, we demonstrate using different spectroscopic tools that indicate the following: (i) DKA reacts with magnesium chloride to give dianionic species; (ii) a complex can be formed involving two cations and two DKA ligand molecules; (iii) the Mn−Mn distance can be deduced from ESR study in the 2:2 complex; (iv) ab initio calculations allowed us to propose two symmetric 2:2 complex structures compatible with the intermetallic distance deduced from experimental data.

Because of its high affinity for Mg^{2+}, DKA may participate through one of its two carboxylate oxygen atoms in the coordination of the metal concomitantly with D64 and D116 aspartic acids (site I). These residues are expected to constitute the site of a 3′-processing reaction of the IN enzyme. This binding may not alter the catalysis of the 3′-processing reaction but could allow the “diketo tweezers” to be localized in the vicinity of the free metal site II (D64 and E152 residues). These tweezers could sequester the second metal ion likely carried into the IN active site by host DNA, thus inhibiting the strand transfer reaction.

DKAs might in fact coordinate magnesium before binding to the active site of IN. This constitutes an important question that should be addressed. We are currently attempting to prepare magnesium complexes in order to test them for their inhibition potency of HIV-1 integrase.

Acknowledgment. This work was financially supported by grants from Le Centre National de la Recherche Scientifique (CNRS) and L'Agence Nationale de la Recherche contre le SIDA (ANRS).

Supporting Information Available: ^1H and ^{13}C NMR spectroscopy conditions, mass spectrometry conditions and mass spectra, and ESR conditions and 9 GHz ESR spectra of Mn^{2+} in the presence of **1** with a metal−ligand ratio of 1/6 in frozen 77 K methanol solution. This material is available free of charge via the Internet at http://pubs.acs.org.

References

(1) Maurin, C.; Bailly, F.; Cotelle, P. Structure−Activity Relationships of HIV-1 Integrase Inhibitors−Enzyme−Ligand Interactions *Curr. Med. Chem.* **2003**, *10*, 1859−1874.

(2) Hazuda, D. J.; Felock, P.; Witmer, M.; Wolfe, A.; Stillmock, K.; Grobler, J. A.; Espeseth, A.; Gabryelski, L.; Schleif, W.; Blau, C.; Miller, M. D. Inhibitors of Strand Transfer That Prevent Integration and Inhibit HIV-1 Replication in Cells. *Science* **2000**, *287*, 646−650.

(3) Goldgur, Y.; Craigie, R.; Cohen, G. H.; Fujiwara, T.; Yoshinaga, T.; Fujishita, T.; Sugimoto, H.; Endo, T.; Murai, H.; Davies, D. R. Structure of the HIV-1 Integrase Catalytic Domain Complexed with an Inhibitor: A Platform for Antiviral Drug Design. *Proc. Natl. Acad. Sci. U.S.A.* **1999**, *96*, 13040−13043.

(4) Wai, J. S.; Egbertson, M. S.; Payne, L. S.; Fisher, T. E.; Embrey, M. W.; Tran, L. O.; Melamed, J. Y.; Langford, H. M.; Guare, J. P.; Zhuang, L.; Grey, V. E.; Vacca, J. P.; Holloway, M. K.; Naylor-Olsen, A. M.; Hazuda, D. J.; Felock, P. J.; Wolfe, A. L.; Stillmock, K. A.; Schleif, W. A.; Gabryelski, L. J.; Young, S. D. 4-Aryl-2,4-dioxobutanoic Acid Inhibitors of HIV-1 Integrase and Viral Replication in Cells. *J. Med. Chem.* **2000**, *43*, 4923−4926.

(5) Marchand, C.; Zhang, X.; Pais, G. C. G.; Cowansage, K.; Neamati, N.; Burke, T. R., Jr.; Pommier, Y. Structural Determinants for HIV-1 Integrase Inhibition by β-Diketo Acids. *J. Biol. Chem.* **2002**, *277*, 12596−12603.

(6) Grobler, J. A.; Stillmock, K.; Hu, B.; Witmer, M.; Felock, P.; Espeseth, A. S.; Wolfe, A.; Egbertson, M.; Bourgeois, M.; Melamed, J.; Wai, J. S.; Young, S.; Vacca, J.; Hazuda, D. J. Diketo Acid Inhibitor Mechanism and HIV-1 Integrase: Implications for Metal Binding in the Active Site of Phosphotransferase Enzymes. *Proc. Natl. Acad. Sci. U.S.A.* **2002**, *99*, 6661−6666.

(7) Pais, G. C. G.; Zhang, X.; Marchand, C.; Neamati, N.; Cowansage, K.; Svarovskaia, E. S.; Pathak, V. K.; Tang, Y.; Nicklaus, M.; Pommier, Y.; Burke, T. R., Jr. Structure Activity of 3-Aryl-1,3-diketo-Containing Compounds as HIV-1 Integrase Inhibitors. *J. Med. Chem.* **2002**, *45*, 3184−3194.

(8) Marchand, C.; Johnson, A. A.; Karki, R. G.; Pais, G. C. G.; Zhang, X.; Cowansage, K.; Patel, T. A.; Nicklaus, M. C.; Burke, T. R., Jr.; Pommier, Y. Metal-Dependent Inhibition of HIV-1 Integrase by β-Diketo Acids and Resistance of the Soluble Double-Mutant (F185K/C280S). *Mol. Pharmacol.* **2003**, *64*, 600−609.

(9) Shaw-Reid, C. A.; Munshi, V.; Graham, P.; Wolfe, A.; Witmer, M.; Danzeisen, R.; Olsen, D. B.; Carroll, S. S.; Embrey, M.; Wai, J. S.; Miller, M. D.; Cole, J. L.; Hazuda, D. J. Inhibition of HIV-1 Ribonuclease H by a Novel Diketo Acid, 4-[5-(Benzoylamino)-thien-2-yl]-2,4-dioxobutanoic Acid. *J. Biol. Chem.* **2003**, *278*, 2777−2780.

(10) Hastings, J. C.; Selnick, H.; Wolanski, B.; Tomassini, J. E. Antiinfluenza Virus Activities of 4-Substituted-2,4-dioxobutanoic Acid Inhibitors. *Antimicrob. Agents Chemother.* **1996**, *40*, 1304−1307.

(11) Summa, V.; Petrocchi, A.; Pace, P.; Matassa, V. G.; De Francesco, R.; Altamura, S.; Tomei, L.; Koch, U.; Neuner, P. Discovery of α,γ-Diketo Acids as Potent Selective and Reversible Inhibitors of Hepatitis C Virus NS5b RNA-Dependent RNA Polymerase. *J. Med. Chem.* **2004**, *47*, 14−17.

(12) Kees, K. L.; Caggiano, T. J.; Steiner, K. E.; Fitzgerald, J. J.; Kates, M. J.; Christos, T. E.; Kulishoff, J. M.; Moore, R. D.; McCaleb, M. L. Studies on New Acidic Azoles as Glucose-Lowering Agents in Obese, Diabetic db/db Mice. *J. Med. Chem.* **1995**, *38*, 617−628.

(13) Maurin, C.; Bailly, F.; Cotelle, P. Improved Preparation and Structural Investigation of 4-Aryl-4-oxo-2-hydroxy-2-butenoic Acids and Methyl Esters. *Tetrahedron* **2004**, *60*, 6479−6486.

(14) Frisch, M. J.; Trucks, G. W.; Schlegel, H. B.; Scuseria, G. E.; Robb, M. A.; Cheeseman, J. R.; Zakrzewski, V. G.; Montgomery, J. A., Jr.; Stratmann, R. E.; Burant, J. C.; Dapprich, S.; Millam, J. M.; Daniels, A. D.; Kudin, K. N.; Strain, M. C.; Farkas, O.; Tomasi, J.; Barone, V.; Cossi, M.; Cammi, R.; Mennucci, B.; Pomelli, C.; Adamo, C.; Clifford, S.; Ochterski, J.; Petersson, G. A.; Ayala, P. Y.; Cui, Q.; Morokuma, K.; Malick, D. K.; Rabuck, A. D.; Raghavachari, K.; Foresman, J. B.; Cioslowski, J.; Ortiz, J. V.; Stefanov, B. B.; Liu, G.; Liashenko, A.; Piskorz, P.; Komaromi, I.; Gomperts, R.; Martin, R. L.; Fox, D. J.; Keith, T.; Al-Laham, M. A.; Peng, C. Y.; Nanayakkara, A.; Gonzalez, C.; Challacombe, M.; Gill, P. M. W.; Johnson, B. G.; Chen, W.; Wong, M. W.; Andres, J. L.; Head-Gordon, M.; Replogle, E. S.; Pople, J. A. *Gaussian 98*, revision A.9; Gaussian, Inc.: Pittsburgh, PA, 1998.

(15) Zouhiri, F.; Mouscadet, J. F.; Mekouar, K.; Desmaële, D.; Savouré, D.; Leh, H.; Subra, F.; Le Bret, M.; Auclair, C.; D'Angelo, J. Structure−activity Relationships and Binding Modes of Styrylquinolines as Potent Inhibitors of HIV-1 Integrase and Replication of HIV-1 in Cell Culture. *J. Med. Chem.* **2000**, *43*, 1533−1540.

(16) Bujacz, G.; Alexandratos, J.; Wlodawer, A.; Merkel, G.; Andrake, M.; Katz, R. A.; Skalka, A. M. Binding of Different Cations to the Active Site of Avian Sarcoma Virus Integrase and Their Effects on Enzymatic Activity. *J. Biol. Chem.* **1997**, *272*, 18161−18168.

(17) Davies, J. F.; Hostomska, Z.; Hostomsky, Z.; Jordan, S. R.; Matthews, D. A. Crystal Structure of the RNase H Domain of HIV-1 Reverse Transcriptase. *Science* **1991**, *252*, 88−95.

(18) Pari, K.; Mueller, G. A.; De Rose, E. F.; Kirby, T. W.; London, R. E. Solution Structure of the RNase H Domain of the HIV-1 Reverse Transcriptase in the Presence of Magnesium. *Biochemistry* **2003**, *42*, 639−650.

(19) Adesokan, A. A.; Roberts, V. A.; Lee, K. W.; Lins, R. D.; Briggs, J. M. Prediction of HIV-1 Integrase/Viral DNA Interactions in the Catalytic Domain by Fast Molecular Docking. *J. Med. Chem.* **2004**, *47*, 821−828.

JM0408464